

**ORIGINAL  
RESEARCH**

N. Ebrahimi  
B. Claus  
C.-Y. Lee  
A. Biondi  
G. Benndorf

# Stent Conformity in Curved Vascular Models with Simulated Aneurysm Necks Using Flat-Panel CT: An In Vitro Study

**BACKGROUND AND PURPOSE:** Radiographic visibility of self-expandable intracranial stents is insufficient for assessment of conformability and deployment characteristics. The purpose of this study was to evaluate stent mechanics in a curved vessel model by using Flat-Panel CT (FPCT).

**MATERIALS AND METHODS:** The following stents were used: Neuroform 2, Neuroform Treo, Enterprise, and LEO. All stents were bent in the same polytetrafluoroethylene tubes with various angles ranging from 150° to 30°. To visualize potential prolapse of the stent struts, 4-, 5-, and 8-mm openings were created. FPCTs were obtained using a C-arm with flat detector.

**RESULTS:** FPCT scans provided excellent visualization of deployment characteristics and stent mechanics and was superior to digital subtraction angiography (DSA) and digital radiography (DR). The Neuroform2/Treo showed, with increasing angle and diameter of the opening, a continuous increase in cell size. These stents also showed an outward prolapse at the convexity and an inwards prolapse of struts at the concavity of the curvature. The Enterprise showed an increasing trend to flatten and to kink with curvatures that are more acute. The LEO showed fewer trends to kink but an inward crimping of its ends with more acute angles.

**CONCLUSIONS:** Deployment characteristics and conformability to a curved vessel model vary considerably, depending on the angle and the stent design. Adverse mechanics such as increased cell opening, strut prolapse, flattening, and kinking occur during stent placement in a curved vessel model, and may gain clinical importance. FPCT is superior to DSA and DR in visualizing small metallic stents and enables accurate detection of adverse stent mechanics.

As a result of recent advancements in endovascular treatment, assisted coiling using self-expanding intracranial stents has become increasingly accepted for treatment of aneurysms.<sup>1-7</sup> Because of their small size, the low radiopacity of nitinol, and the overlying bony structures when they are placed close to the skull base, radiographic visualization of these stents is poor. To compensate for this lack of visibility and to facilitate fluoroscopic control during positioning, manufacturing companies have added highly radiopaque platinum markers at the end of the stents. The stent body itself, however, is usually not identifiable and thus assessment of deployment and conformability to curved vasculature or the detection of adverse stent mechanics using nonsubtracted digital radiography (DR) remains unsatisfactory. Flat-panel CT (FPCT) has been proven to considerably enhance image quality of intracranial stents.<sup>8,9</sup> The purpose of this study was to evaluate conformability and deployment characteristics of currently available self-expanding stents in a curved vessel model by using FPCT compared with fluoroscopy and DR.

## Materials and Methods

To study deployment characteristics and conformability to curved vessels, 4 self-expanding stents currently available for use in intracranial vessels were used (Table 1).

Received June 7, 2006; accepted after revision August 14.

From the Biomechanical Engineering Program (N.E.), University of Houston, Houston, Tex; the Department of Cardiovascular Surgery (B.C.), Charite, Humboldt University, Berlin, Germany; the Department of Neuroradiology (A.B.), Pitie-Salpetriere Hospital, Paris, France; and the Department of Radiology (C.-Y.L., G.B.), The Methodist Hospital Houston.

Paper previously presented at the 44th Annual Meeting of the American Society of Neuroradiology; April 29–May 5, 2006; San Diego, Calif.

Address correspondence to G. Benndorf, MD, PhD, Department of Radiology, The Methodist Hospital, 6565 Fannin, Houston, TX 77030; e-mail: gbenndorf@tmh.tmc.edu

The 2 open-cell design intracranial stents, Neuroform2 Stent (NF2) and Neuroform Treo-Stent (NF3) (Boston Scientific, Natick, Mass) used in this study, are both made of a nickel-titanium alloy (nitinol) with a similar design defining the structure of struts, cells, and markers. The difference between the 2 stents is that the NF Treo has 3 connecting elements along the circumference and the NF2 has only 2 such connectors. Both stents have 4 platinum markers at each end, facilitating their radiographic visualization during deployment under fluoroscopy.

The Enterprise Stent (Cordis, Miami Lakes, Fla) is a nitinol stent with a closed-cell design and 4 platinum markers, each located on a different plane of the flared ends of the stent.

The LEO Stent (Balt Extrusion, Montmorency, France) consists of braided nitinol wires that slide onto each other when bent. This stent, currently unavailable in the United States, has 2 longitudinal platinum wires intertwined as markers to ensure radiographic visibility.

Polytetrafluoroethylene tubes (PTFE, WL Gore & Associates, Newark, Del), 4 mm × 10 cm and 3 mm × 10 cm, were used as models (Fig 1B). To simulate an aneurysm neck and to assess adverse mechanics such as outward prolapse of struts, 4-, 5-, and 8-mm holes were punched into 3 separate PTFE tubes by using an arteriotomy device. Under fluoroscopic guidance, each stent was deployed in the midsection of a PTFE tube that was then placed onto a styrofoam block and stepwise bent in angles ranging from 150° to 30° (150°, 120°, 90°, 75°, 60°, 45°, and 30°) (Fig 1A, -B).

For each bending, rotational radiograms were performed using a single C-arm angiographic system with an 20 × 20-cm CsI/amorphous Silicon flat detector (Axiom Artis dFC; Siemens Medical Solutions, Erlangen, Germany) with the following parameters: 11 seconds, 0.8° increment, and 273 projections. In addition, nonsubtracted digital radiographic (DR) images were obtained for comparing the radiopacity of the different stents. FPCT scans (DynaCT; Siemens Medical Solutions) were

**Table 1: Self-expanding intracranial stents**

Stent	Material	Design	Diameter (mm)	Length (mm)	Manufacturer
Neuroform2	Nitinol	Open cell	4.0	25.0	Boston Scientific
Neuroform-Treo	Nitinol	Open cell	3.5	20.0	Boston Scientific
Enterprise	Nitinol	Closed cell	4.0 ± 0.5	22.0	Cordis
LEO	Nitinol	Braided wires	4.5 ± 0.5	25.0 ± 2.0	Balt Extrusion

obtained by performing 3D reconstructions with the use of a dedicated, commercially available workstation (Leonardo; Siemens). Reconstructions of the stents were done using manual mode, choosing minimal voxel size (smallest distinguishable box-shaped part of a 3D image) ranging from 0.08 to 0.04 mm, and a 512 × 512 reconstruction matrix. Thin-section maximum intensity projections (MIPs; 1 mm) were used to obtain “in-stent” views and cross-sectional (orthogonal) views of the stent lumen. For postprocessing, the images were viewed in volume-rendered technique (VRT), as multiplanar reconstructions or MIPs.

## Results

The radiographic visualization of all 4 stents under fluoroscopy or DR was insufficient to demonstrate the stent structure itself or adverse mechanics caused by the bending (Fig 2). Only the LEO stent was visualized over its entire length because of its longitudinal markers. Reliable detection of strut prolapse into a 8-mm opening (simulated “aneurysm neck”) using fluoroscopy or DR was not possible.

FPCT provided visualization of all stents in high quality and was found to be superior to DR in visualizing the entire stents, including struts and cells. It showed details of the stent architecture, allowing for evaluation of deployment and conformability of the stents when bent in various degrees. The reconstructions allowed interactive rotation of the stent, revealing structural details in every possible plane, including orthogonal (“down the barrel”) projections and *en face* views onto the stent cells. MIPs were the most preferable mode and allowed for differentiation between stent portions with different radiopacity such as struts and connecting elements, made of nitinol, and the platinum stent markers. FPCT allowed detection of adverse stent mechanics in all 4 stent types, particularly when using thin sections to obtain “in stent” views (Fig 3).

The use of the PTFE tubes provided high-quality 3D reconstructions with only minimal artifacts, which allowed us to precisely study the stent behavior across the simulated “aneurysm necks.” Table 2 gives an overview of the stent mechanics seen with different degrees of bending.

### Neuroform2 Stent

Already at 0° curvature (straight tube), the NF2 (Figs 3 and 4), with only 2 connectors per circumference, showed a minor asymmetric deployment across the 4-, 5-, and 8-mm openings. In each model, the stent cells demonstrated continuously increased opening, as well as an outward prolapse of the struts at the convexity of the models into the simulated “aneurysm necks,” with increasing the bends. At the concavity, an inward prolapse of struts starting at 75° was documented using thin-section MIPs, increasing with more acute curvatures. Good apposition of the stent struts to the wall of the tubes with the simulated “aneurysm necks” was observed only at the distal and proximal ends with the markers in correct positions. Op-

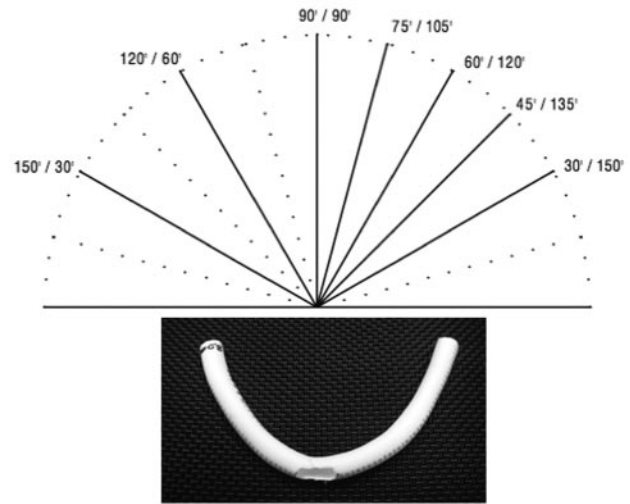


**Fig 1.** A, Angles of bending from 180° (0°) to 30° (inner angle of model curve).

B, PTFE tube, 4-mm diameter with 8-mm opening as used for stent deployment and bending.

timal deployment and apposition of the stent struts to the PTFE tube with no opening was observed, along with only a minor inward prolapse of struts at the concavity starting at 75° curvature.

### Neuroform Treo Stent

Because of its similar design, the NF3 showed a behavior very similar to the NF2 (Fig 5). At 0° (180°) curvature, a minor asymmetric deployment of the stent within the tubes with 4-, 5-, and 8-mm openings was documented. The cells showed a continuously increased opening with decreasing the inner angle of the bend (more acute curvature), as well as an outward prolapse of the struts at the convexity, similar to the NF2. In addition, continuous cell opening at the distal and proximal end of the stent was found, increasing in size with decreasing of the angle of the bend.

At the concavity, an inward prolapse of the struts, starting at 75°, was documented using thin-section MIPs, with an increasing trend, as the angles were made smaller. A trend of loss of normal configuration of stent struts was observed starting at 75° bend.

### Enterprise Stent

The Enterprise showed no cell openings as the NF2 and NF3 stents did (Fig 6). Starting at the 90° bend, the Enterprise revealed minor kinks and flattening at the midsection, increasing with greater bends. It was also evident that as the size of the aneurysm neck increased, the Enterprise tended to flatten and to kink even more at the concavity of the curvature. There was a difference in the degree of kinking of the stent struts in the various PTFE models. In the PTFE tubes with the 4- and 5-mm simulated “aneurysm necks,” the stent started to kink. This tendency seemed to be more evident as the “aneurysm neck” increased from 4 to 5 mm but was not as apparent between the 5- and 8-mm holes, and the degree of flattening and kinking of the stent struts remained relatively the same. Although the cross-sectional area of the midsection of the stent changed significantly during the bending from round to oval and 1 diameter became very small, the stent did not completely collapse.

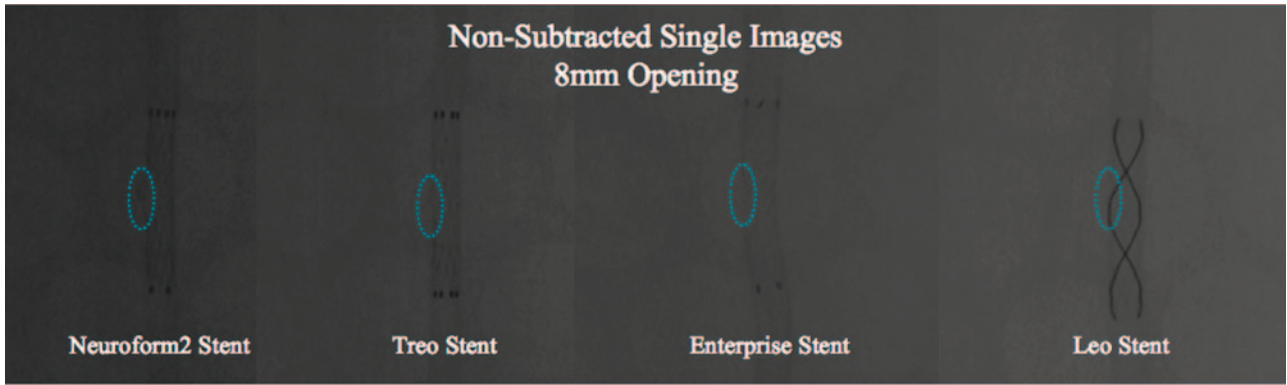


**Fig 2.** Nonsubtracted digital radiography (DR) images of the stents. The DRs of the Neuroform2 and Neuroform2-Treo stents visualize the proximal and distal platinum markers clearly; however, the structure of the stent cells and struts is poorly defined. The Neuroform2 image shows only faintly the prolapse of the struts at the site of the 8-mm opening (*dotted blue ellipse*). This phenomenon seems to occur to a lesser degree with the Neuroform-Treo stent because of the one extra connector along the circumference of the stent, reducing the area of open cells by about 39%. The Enterprise stent is only visualized by its proximal and distal platinum markers. The stent cells and struts are not defined because of the small size of the stent struts ( $50 \times 50 \mu\text{m}$ ); therefore, the structural details of stent are not visible. The LEO stent is seemingly better visualized throughout its entire length, outlined by 2 platinum wires intertwined along the surface of the stent serving as markers; the stent cells and struts, however, are not identifiable.

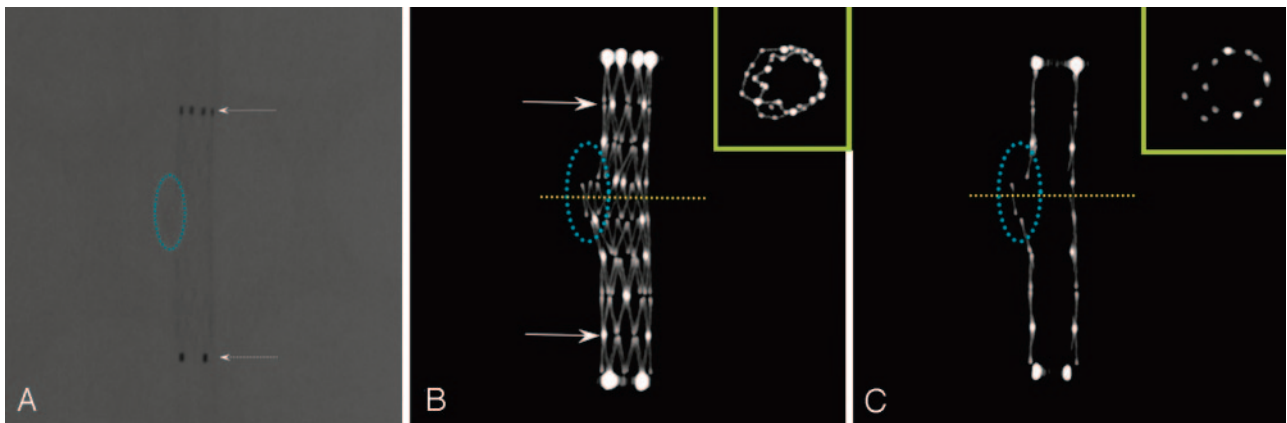


**Fig 3.** Neuroform2, DR and FPCT (MIPs). To increase flexibility and conformability, this stent has an open-cell design with 2 connectors per circumference. The DR shows the proximal and distal markers well (A, *dotted arrows*); however, the stent cells and struts are poorly defined. FPCT using multiplanar reconstructions or MIPs is superior in displaying the stent architecture in detail, allowing for differentiation between struts, connectors (seen as 2 moderately bright spots per circumference, C, *arrows*) as well as the platinum markers. Thin sections allow an “in-stent” view and clearly show the protrusion of stent struts through a 5-mm hole (“aneurysm neck,” *dotted blue ellipse*). This prolapse is difficult if not impossible to identify when using DR or fluoroscopy. FPCT makes it also possible to obtain cross sections of the stent lumen at the level of the opening, creating a *double lumen* figure (C, *miniature yellow box*).

**Table 2: Summary of the results**

	Deployment	Configuration	Strut Characteristics
Neuroform2	Asymmetric	Increased opening of stent cells with decreasing angle	Inward and outward prolapse of the stent struts starting at $110^\circ$ curve
Neuroform-Treo	Asymmetric	Increased cell opening of the stent with decreasing angle (less than NF2)	Less outward prolapse but more inward prolapse of the struts than NF2 with decreasing angles, starting at $75^\circ$
Enterprise	Symmetric	Loss of normal strut configuration starting at $110^\circ$ curve Change of shape from round to oval Reduction of the stent diameter at the midsection starting at $90^\circ$	Increasing trend to flatten and to kink at the concavity with increasing size of the “aneurysm neck”
LEO	Symmetric	Flattening of the midsection of the stent starting at $90^\circ$ Flattening and narrowing of the distal and proximal ends starting at $115^\circ$	Less tendency to kink and flatten than Enterprise Inward crimping of proximal and distal ends with lumen narrowing

### LEO Stent

The LEO (Fig 7) demonstrated a symmetric deployment in all 4 PTFE tube models for the first degrees of bend, ranging from  $0^\circ$  to  $120^\circ$  (inside angles). Starting at  $115^\circ$  bend, the distal and proximal ends of the stent tended to flatten as the degree of bending was increased. The MIPs demonstrated a flattening of the stent at the midsection starting at  $90^\circ$ . This phenomenon tended to be more evident with increasing size of the simulated aneurysm necks;

however, there was no tendency to kink or collapse as seen with the Enterprise. Furthermore, at  $30^\circ$ , a significant inward crimping of the proximal stent ends became visible.

### Discussion

Although recent advancements in endovascular techniques have led to a significant increase of using intracranial stents for aneurysm treatment,<sup>2-6,10-15</sup> the conformability and deploy-

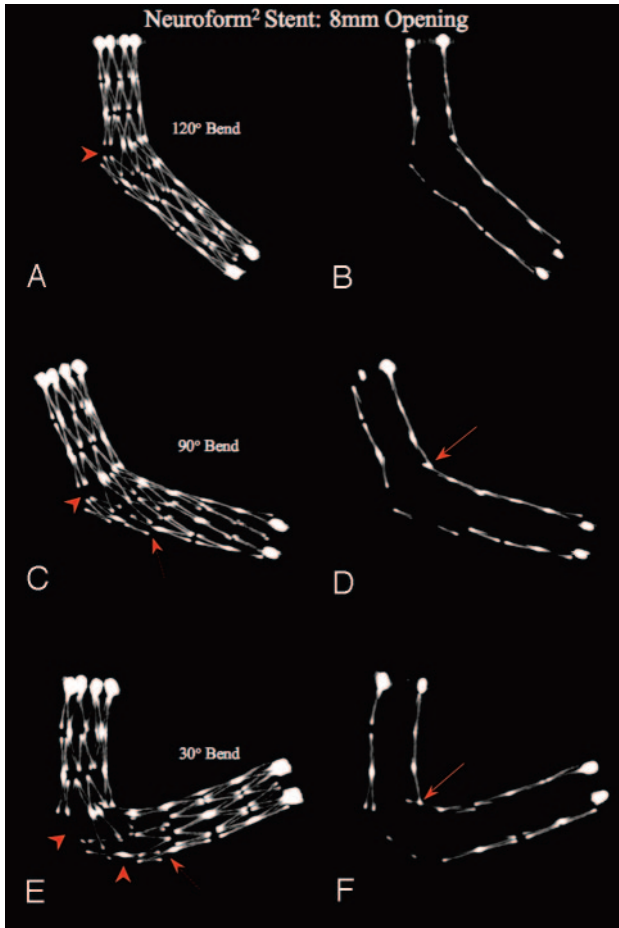


**Fig 4.** Neuroform2 Stent: constant opening, increasing bend. MIPs, using section thickness of 1.0 mm (right column) and 5.0 mm (left column), bending with 120°, 90°, and 30° angles, over a simulated “aneurysm neck” (8-mm hole in the PTFE tube, dotted blue ellipse in the left column). The MIPs demonstrate an asymmetric deployment of the stent at the site of the hole. As the angle of the bend decreases, there is an increased opening of the stent cells, along with a tendency of the stent struts to protrude more into the aneurysm cavity (arrowheads). Using 1.0-mm section MIPs, starting at the 90° bend, a minor inward prolapse of the stent struts at the concavity (arrows) occurs. These findings are not detectable using current conventional radiographic techniques such as fluoroscopy or DR.

ment characteristics of the currently available self-expanding intracranial stents to curved vasculature have not been studied extensively. Numerous recent publications rely on information gained with the use of DSA or DR to assess efficiency and conformability of self-expanding stents without sufficient image information to truly support this.

The tenuous properties of these stents provide highly flexible characteristics for better apposition in the tortuous intracranial vascular anatomy. However, their radiopacity is limited and their visualization decreased when using conventional radiographic techniques, such as DSA and/or DR. Except for the LEO, the main body of the nitinol stents currently on the market is usually not visible under fluoroscopy in clinical practice, not even during more ideal experimental conditions. Even though the LEO is made more radiopaque by adding 2 longitudinal platinum markers, the nitinol wires building the stent struts are not visualized enough to fully appreciate the stent body. Assessment of degree and symmetry of deployment as an indirect indicator for good wall apposition is therefore difficult, if not impossible. This is particularly true when placed intracranially where

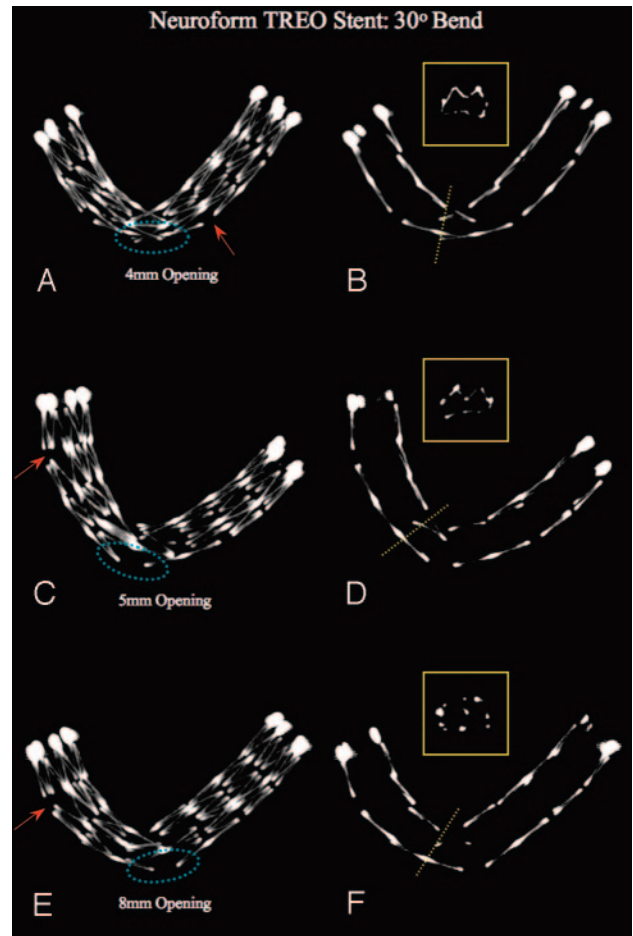


**Fig 5.** Neuroform-Treo Stent: constant bend 30°, increasing size of openings (“aneurysm necks”). MIPs using section thickness of 5.0 mm (left column) and 1.0 mm (right column), bending with 30° angle over 4-, 5-, and 8-mm holes or simulated “aneurysm necks” (left column, dotted blue ellipse). As compared with the NF2 stent, the NF3 shows less increase in cell opening with increased bend, probably because of the presence of one or more connectors per circumference. Some minor increase in opening can be seen remote from the curvature (arrows). The thin-section MIPs show an increased inward prolapse of struts into the stent lumen as the diameter of the holes increases. This seems more pronounced compared with the NF2. However, whether this phenomenon occurs also depends on the positioning of the stent relative to the location of the “aneurysm neck.” In the absence of a connector across the opening, the stent struts still protrude into the “aneurysm,” though to a lesser degree than seen with NF2. Miniatures (yellow boxes, left column): Cross-sectional view of the inner stent lumen at its midsection.

overlying bony structures compromise radiographic visualization.

Imaging of small intracranial stents using alternative modalities such as MR imaging is limited as a result of the lower spatial resolution and susceptibility artifacts to the blood flow proximal and distal to the stent. CT combined with CTA has been used to visualize coronary arteries and coronary stents. However, these do not provide detail resolution equal to FPCT.<sup>16</sup> Maintz et al<sup>16</sup> reported on an in vitro study of 68 different coronary stents using state-of-the-art 64 multidetector row CT obtaining a minimum section thickness of 0.6 mm. The authors state that even with the improved spatial resolution of the latest generation CT scanner, stent-optimized reconstructions remain necessary.

Akpek et al<sup>17</sup> reported on the value and potential of 3D and cross-sectional imaging using a new C-arm with flat detector for various applications. Because modern flat detectors on ro-

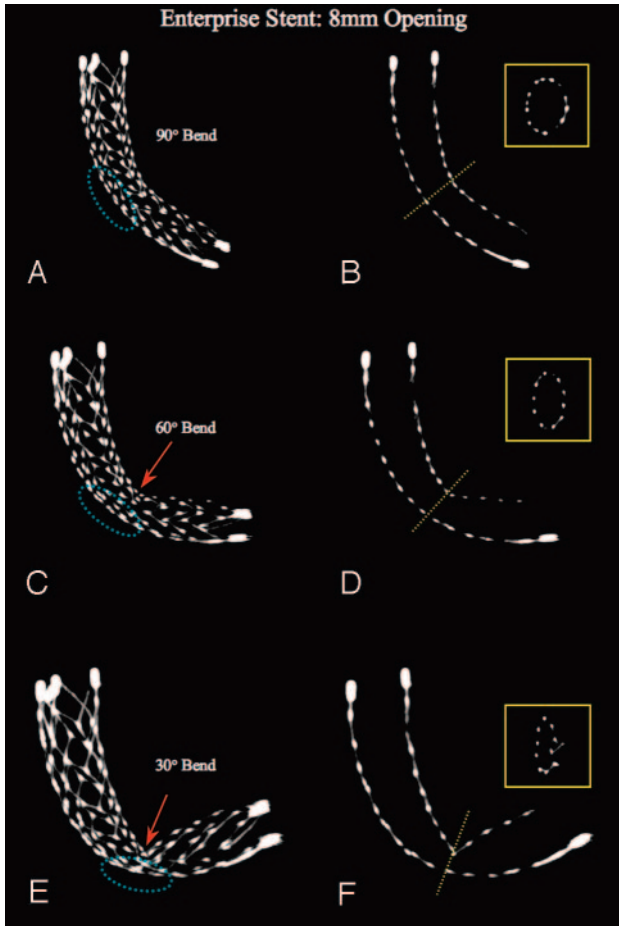


**Fig 6.** Enterprise Stent: constant 8-mm opening, increasing bend. MIPs, using section thickness of 5.0 mm (*left column*) and 1.0 mm (*right column*), bending with 90°, 60°, and 30° angles, over a 8-mm hole simulated “aneurysm neck” (*dotted blue ellipse*). It is evident that starting from a 90° bend, the Enterprise stent shows initially a minor flattening at its midsection that increases with 60° and becomes a true kinking at 30°. It also documents that the stent tends not to completely collapse, even though the midsection of the stent significantly changes its shape from round to oval and the diameter becomes relatively small (*miniatures*).

tating C-arms, such as used in this study, are capable of providing a true isotropic resolution of 0.1 mm, they are capable of generating 3D reconstructions of small metallic stents with image quality superior to that obtained by other currently available clinical imaging modalities. The spatial resolution of the detector used in this study is less than 200  $\mu\text{m}$  (a detector element on a 20  $\times$  20-cm FD is 184  $\mu\text{m}$ ), allowing for visualization of stents with a strut size ranging from approximately 50 to 70  $\mu\text{m}$ .

The relatively high contrast of a metal structure and a contributing partial volume effect enhances the attenuation, providing a radiographic visibility that cannot be matched by other current clinical imaging modalities. It makes FPCT a promising new tool for imaging of small metallic stents *in vitro* as well as *in vivo*.<sup>8</sup> As shown, FPCT allows identification and better understanding of deployment characteristics and conformability of these stents. This becomes particularly important in tortuous or curved vasculature, where the 3D volumes can be interactively rotated to obtain an orthogonal or “in-stent” view in every possible plane. Further improvement of FPCT using faster reconstruction algorithms and kernels,

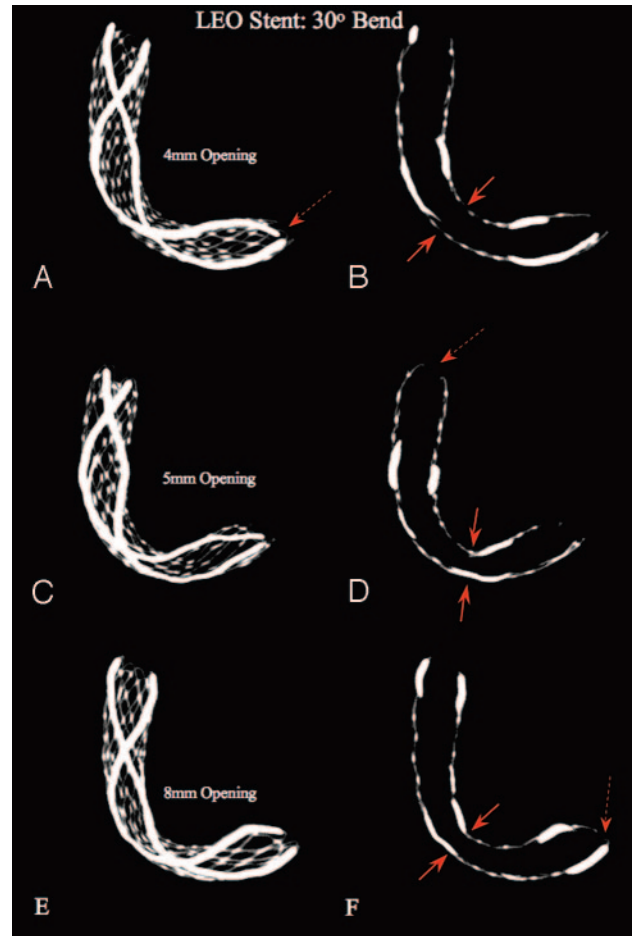


**Fig 7.** LEO Stent: constant bend, increasing size of openings (“aneurysm necks”). MIPs using section thicknesses of 5.0 and 1.0 mm, bending with 30° angle, in 4-, 5-, and 8-mm simulated aneurysm necks. The MIPs show that as the size of the holes (“aneurysm necks,” *dotted blue ellipse*) increases, the stent tends to flatten more at its midsection (*arrows*), whereas the degree of bending is unchanged. This phenomenon seems more pronounced if the platinum markers do not cross the aneurysm neck, hence the nitinol wires are thinner and softer. The MIPs further demonstrate an inward crimping of the proximal and distal ends, significantly narrowing the lumen of the stent at these points (*double arrows*).

specifically developed for stent reconstruction, is expected in the near future and is the topic of an ongoing study.

The results of our study show that the conformability of currently available intracranial self-expanding nitinol stents with closed- and open-cell designs to curved vasculature differs significantly. The lack of conformability to the extracranial carotid bifurcation has been studied by Tanaka et al<sup>18</sup> with the use of a silicon model. The authors found that segmented stent design, also called open-cell design, conforms better to vascular tortuosities.

As demonstrated here, an open-cell design stent, such as the NF2 and NF3, adapts well to a native curved vessel contour because of their segmented geometry. However, the stents may show increased opening of cells and outward prolapse of struts into an aneurysm neck when situated at the convexity of the curvature, whereas at the concavity, struts, or stent segments may protrude inward. The hemodynamic effects of these adverse phenomena are unknown so far but may contribute to adverse effects, such as stent thrombosis or in-stent stenosis. In curved vessels harboring an aneurysm at the convexity, an increased cell opening may facilitate untoward her-

niation of coils into the stent lumen (parent vessel lumen). This may become important during endovascular treatment, particular when using coils smaller than the usual cell size (largest opening = 4.36 mm<sup>2</sup> in a 4.5-mm vessel, according to the manufacturer). Even with slightly larger coils, this may happen when the number of struts bridging the neck provides insufficient scaffolding. The use of 3D coils or other complex coils may be advisable to cover the area with too much cell opening first. The inward prolapse of struts at the concavity of the curvature may impair the possibilities of entering an aneurysmal neck when located at this side of the curvature.

Any vessel curve ranging from 30° to 150°, particularly an acute vessel turn as is frequently present in the carotid siphon, requires the stent to adapt to the vasculature with a shortening of its lengths at the concavity causing the inward prolapse of the stent struts. This is assured by the segmented design, where cells may slide and overlap onto each other, the major advantages of an open-cell design stent. Nevertheless, it should be kept in mind that this overlap of cells and struts causes to some degree a protrusion of stent material into the lumen, representing not only a potential source of thromboemboli but also a source of entanglement with coils, guidewires, microcatheters, or other devices. Such adverse mechanical effects were observed by our group in a clinical case of NF2 stent placement with no clinical consequences.<sup>8</sup>

A stent with a closed-cell design, such as the Enterprise, will maintain a constant cell opening at the convexity of a vessel curve, and protrusion of stent segments outside the parent vessel lumen or into an aneurysm neck is unlikely to occur. In a small clinical case series, no adverse stent mechanics or related clinical consequences during and after stent placement were reported.<sup>12</sup> However, when a closed-cell design is bent, it has, in principle, less flexibility to conform to a curved or irregular anatomy. The unsegmented design does not allow the stent to lengthen at the outer curve or to shorten at the inner curve. This limitation in adapting to a vessel curvature will cause flattening of the stent or, as seen in our study, in very acute curves, even a kinking or buckling. Buckling of self-expanding nitinol stents may occur, albeit less often than with balloon-expanding stainless steel stents. It might become important when considering long-term effects such as fatigue damage although a material such as nitinol has proved otherwise, performing better than any other known metal.<sup>19</sup> As seen in our study, the buckling may increase not only with more acute curves but also as the width of the aneurysm neck increases. The effects might limit to some degree the use of this stent in vessels with acute curves such as the carotid siphon, the anterior communicating artery, or when bridging from the P1 to the basilar artery.

In theory, the LEO represents a hybrid stent, because its structure is neither a real closed- nor an open-cell design. It is made of braided nitinol wires that are woven into a flexible mesh allowing a symmetric deployment of the stent even in sharp vessels turns. Because the wires can basically “slide” onto each other, its advantage lies in its very adjustable structure conforming well to the given anatomy. In theory, the cells at the outer curve can enlarge while the ones at the inner curve become smaller. The main drawback of this less rigid design may lie in the possibility of its being deformed while deployed or when a microcatheter has to be advanced through its lumen

or through its cells. This stent performed well in a curved vessel model with no prolapse and less tendency to buckle or kink than the Enterprise. However, we have documented an inward crimping of the stent ends during the bending that seems to be caused by the intertwined platinum wires and may cause malposition of the stent ends as well as a narrowing of the effective stent lumen. This effect is possibly caused by the longitudinal orientation of the platinum wires that cannot adjust to the different length of the inner and outer curve. Even though the body of the LEO is not fully visible under fluoroscopy, its longitudinally intertwined platinum marker wires allow a relatively more complete visualization compared with the stents with end markers only. As reported recently,<sup>2,4,6</sup> this stent proved feasible and safe in clinical practice for endovascular treatment of aneurysms.

Several limitations of this study need to be considered. The PTFE tube used modeled only an ideal vessel anatomy with consistent 3- or 4-mm diameter. Therefore, the results obtained do not correspond to vessels with varying diameters or diseased, irregular, or calcified walls. The vessel curves in the cerebral circulation, in particular in the carotid siphon, often follow a 3D course, not 2 dimensions only, as simulated in our study. Consequently, some of the adverse mechanics might be exaggerated or underestimated compared with in vivo situations. Another limitation of our study is that only one model was used per stent type (because of limited resources), and not all stents were exactly the same size. However, we believe this would not significantly affect the results of our study. Silicone and glass aneurysm models have been widely used for vascular models for in vitro studies of stents because of their transparency allowing for direct visualization.<sup>18</sup> These models, however, lack mechanical properties similar to human vessels. The use of PTFE tubes is advantageous because of its soft and elastic properties, resembling normal human arteries. In addition, after conducting initial experiments using silicon tubes, we found that PTFE caused significantly less reconstruction artifacts, providing higher image quality for visualization of structural stent details.

## Conclusions

Currently available designs of self-expanding stents are not ideal and may cause several adverse mechanics when deployed in curved vessel models. FPCT provided very detailed 3D visualizations of structural details of such stents. It represents a novel imaging tool allowing for cross-sectional and “in-stent” evaluation of normal and abnormal deployment characteristics of small metallic stents. Therefore, FPCT will contribute to our understanding of stent mechanics in clinical practice, particularly when using small intracranial stents in neurovascular procedures.

## References

1. Fiorella D, Albuquerque FC, Han P, et al. Preliminary experience using the Neuroform stent for the treatment of cerebral aneurysms. *Neurosurgery* 2004; 54:6–16; discussion 16–17
2. Kis B, Weber W, Berlit P, et al. Elective treatment of saccular and broad-necked intracranial aneurysms using a closed-cell nitinol stent (Leo). *Neurosurgery* 2006;58:443–50
3. Lee YJ, Kim DJ, Suh SH, et al. Stent-assisted coil embolization of intracranial wide-necked aneurysms. *Neuroradiology* 2005;47:680–89
4. Lubicz B, Leclerc X, Levivier M, et al. Retractable self-expandable stent for

- endovascular treatment of wide-necked intracranial aneurysms: preliminary experience. *Neurosurgery* 2006;58:451–57
5. Lylyk P, Ferrario A, Pasbon B, et al. **Buenos Aires experience with the Neuroform self-expanding stent for the treatment of intracranial aneurysms.** *J Neurosurg* 2005;102:235–41
  6. Pumar JM, Blanco M, Vazquez F, et al. **Preliminary experience with Leo self-expanding stent for the treatment of intracranial aneurysms.** *AJNR Am J Neuroradiol* 2005;26:2573–77
  7. Sani S, Jobe KW, Lopes DK. **Treatment of wide-necked cerebral aneurysms with the Neuroform2 Treo stent. A prospective 6-month study.** *Neurosurg Focus* 2005;18:E4
  8. Benndorf G, Claus B, Strother CM, et al. **Increased cell opening and prolapse of struts of a Neuroform stent in curved vasculature: value of angiographic computed tomography: technical case report.** *Neurosurgery* 2006;58:ONS-E380; discussion ONS-E380
  9. Benndorf G, Strother CM, Claus B, et al. **Angiographic CT in cerebrovascular stenting.** *AJNR Am J Neuroradiol* 2005;26:1813–18
  10. Chow MM, Woo HH, Masaryk TJ, et al. **A novel endovascular treatment of a wide-necked basilar apex aneurysm by using a Y-configuration, double-stent technique.** *AJNR Am J Neuroradiol* 2004;25:509–12
  11. Fiorella D, Albuquerque FC, Deshmukh VR, et al. **Usefulness of the Neuroform stent for the treatment of cerebral aneurysms: results at initial (3–6-mo) follow-up.** *Neurosurgery* 2005;56:1191–201; discussion 1201–02
  12. Higashida RT, Halbach VV, Dowd CF, et al. **Initial clinical experience with a new self-expanding nitinol stent for the treatment of intracranial cerebral aneurysms: the Cordis Enterprise stent.** *AJNR Am J Neuroradiol* 2005;26:1751–56
  13. Horowitz M, Levy E, Sauvageau E, et al. **Intra/extra-aneurysmal stent placement for management of complex and wide-necked bifurcation aneurysms: eight cases using the waffle cone technique.** *Neurosurgery* 2006;58:ONS-258–262
  14. Perez-Arjona E, Fessler RD. **Basilar artery to bilateral posterior cerebral artery ‘Y stenting’ for endovascular reconstruction of wide-necked basilar apex aneurysms: report of three cases.** *Neurol Res* 2004;26:276–81
  15. Wanke I, Doerfler A, Schoch B, et al. **Treatment of wide-necked intracranial aneurysms with a self-expanding stent system: initial clinical experience.** *AJNR Am J Neuroradiol* 2003;24:1192–99
  16. Maintz D, Seifarth H, Raupach R, et al. **64-slice multidetector coronary CT angiography: in vitro evaluation of 68 different stents.** *Eur Radiol* 2006;16:818–26
  17. Akpek S, Morsi H, Benndorf G, et al. **Reconstruction of the basilar tip with T stent configuration for treatment of a wide-neck aneurysm.** *J Vasc Interv Radiol* 2004;15:1024–26
  18. Tanaka N, Martin JB, Tokunaga K, et al. **Conformity of carotid stents with vascular anatomy: evaluation in carotid models.** *AJNR Am J Neuroradiol* 2004;25:604–07
  19. Duerig T, Wholey M. **A comparison of balloon and self-expanding stents.** *Min Invas Ther Allied Technol* 2002;(4):173–78